

Supplementary information for:

Investigation of the interactions between organophosphorous agents and TiO₂ modified microcantilevers for molecule detection in air

Urelle Biapo,^{a*} Denis Spitzer,^b Valérie Keller,^a Philippe Bazin^c and Thomas Cottineau^{a*}

XPS

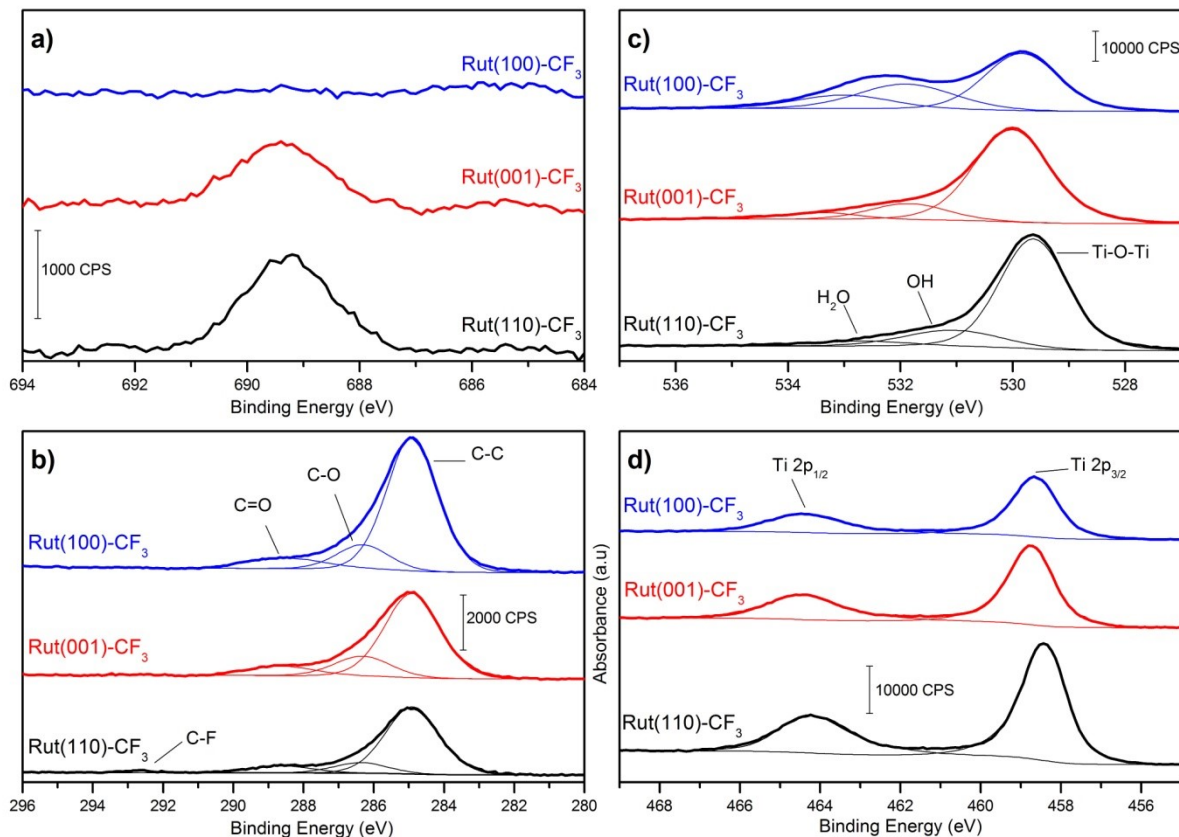


Figure S1: XPS analysis of (100), (001) and (110) rutile monocrystals modified with Fluorine molecules : (a) F 1s
(b) C 1s, (c) O 1s and (a) Ti 2p peaks.

Table S1: XPS deconvolution parameters for the (100), (001) and (110) rutile monocrystals modified with Fluorine molecules.

		Attribution	Position (eV)	FWHM (eV)	R.S.F.	At conc. %	
Rutile (001) CF₃							
C 1s	A	C-C	284.9	1.81	1.00	22.3	32.0
	B	C-O	286.2	1.81	1.00	5.9	
	C	C=O	288.6	2.50	1.00	3.8	
F 1s		C-F	688.5	2.01	4.43	1.4	1.4
O 1s	A	Ti-O	530.0	1.60	2.93	42.6	53.0
	B	-OH	531.9	1.60	2.93	7.3	
	C	-H ₂ O	533.4	1.60	2.93	3.1	
Ti 2p_{3/2}		Ti-O	458.7	1.28	5.22	13.6	13.6
Rutile (100) CF₃							
C 1s	A	C-C	284.9	1.71	1.00	29.9	39.3
	B	C-O	286.3	1.71	1.00	5.6	
	C	C=O	288.5	2.71	1.00	3.8	
F 1s		C-F	688.6	1.67	4.43	0.2	0.2
O 1s	A	Ti-O	529.9	1.55	2.93	26.7	49.5
	B	-OH	531.9	2.00	2.93	14.8	
	C	-H ₂ O	533.0	2.00	2.93	8.0	
Ti 2p_{3/2}		Ti-O	458.6	1.27	5.22	10.7	10.7
Rutile (110) CF₃							
C 1s	A	C-C	284.9	1.83	1.00	15.7	20.0
	B	C-O	286.4	1.83	1.00	2.3	
	C	C=O	288.6	1.98	1.00	1.7	
	D	C-F	292.7	0.93	1.00	0.3	
F 1s		C-F	688.3	1.97	4.43	1.8	1.8
O 1s	A	Ti-O	529.7	1.41	2.93	45.6	57.8
	B	-OH	531.1	2.00	2.93	9.4	
	C	-H ₂ O	532.7	2.00	2.93	2.9	
Ti 2p_{3/2}		Ti-O	458.4	1.27	5.22	20.4	20.4

DMMP detection curves

The μ cantilever frequency shift associated to DMMP adsorption and desorption were fitted by a biexponential decay functions.

$$\Delta f_{ads} = \Delta f_0 + A_1 e^{-\frac{x-x_0}{t_1}} + A_2 e^{-\frac{x-x_0}{t_2}}$$

Single exponential function cannot reproduce correctly the curves. This suggests that two different phenomena govern the absorption kinetics. (A_1 , t_1) and (A_2 , t_2) are the constant associated to these phenomena and our hypothesis is that the fast transition is associated with physical adsorption/desorption at the film surface while the slower one is related to chemical interaction with the surface and diffusion in the porosity of the TiO_2 -NRs films. All fitting were done with Origin program. Figure S2 gives an example of data fitting for the pristine TiO_2 nanorods. The constants extracted for the different samples are gathered in table S2.

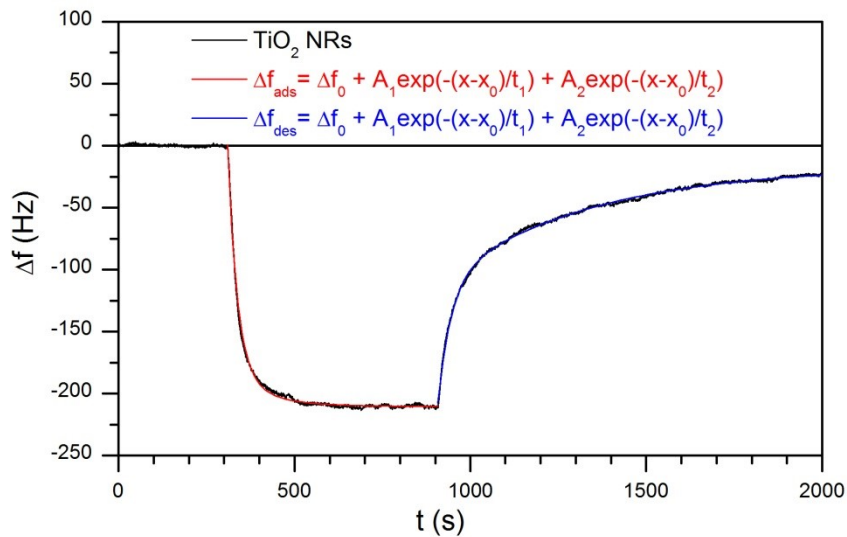


Figure S2: Example of fitting of the frequencies shift curves during the DMMP absorption / desorption on the microcantilever.

Table S2: Fit parameters of the frequency shifts during DMMP absorption/desorption for the μ cantilevers modified with different molecules.

	Δf_{10min} (Hz)	Adsorption					Desorption	
		A_1 (Hz)	t_1 (s)	A_2 (Hz)	t_2 (s)	A_1+A_2 (Hz)	t_1 (s)	t_2 (s)
TiO_2	-210.0	183.0	27.3	27.8	103.1	210.8	37.2	419.0
Fluorine	-312.0	216.0	26.4	98.0	30.8	314.0	25.7	118.9
Oxime	-372.0	238.3	19.6	151.8	235.5	390.1	32.6	352.7
Amine	-604.0	260.6	36.8	386.8	238.3	647.4	73.9	499.8

In situ TDP followed by IR measurements.

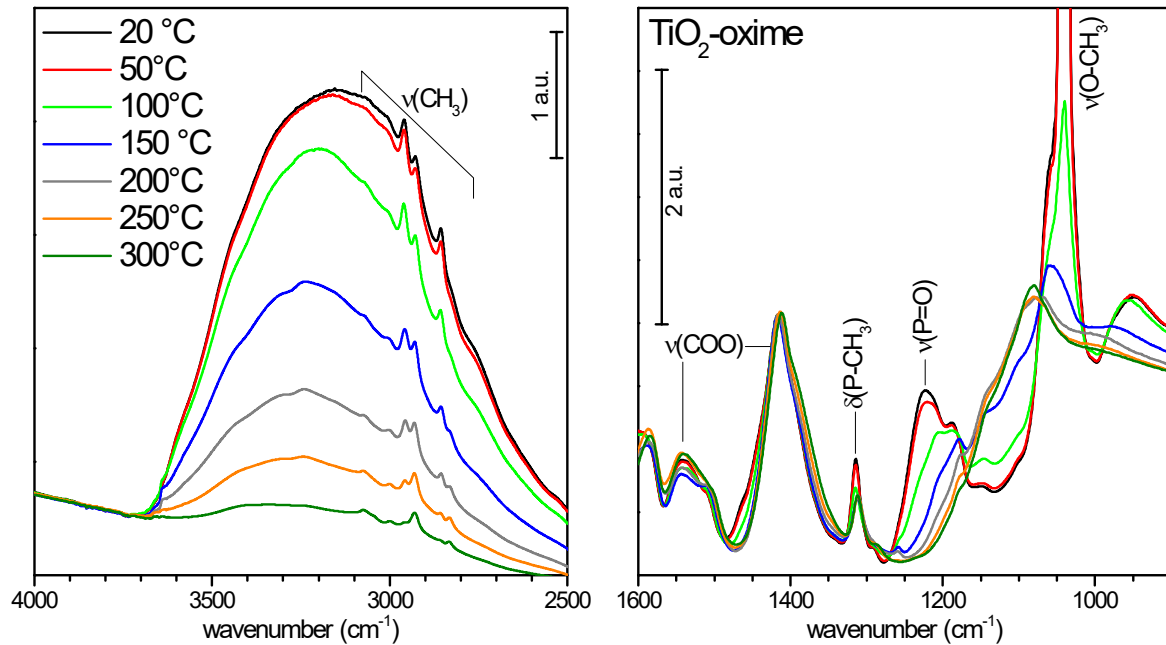


Figure S3: IR patterns of TiO_2 -oxime recorded during the thermal programmed desorption between 20 and 300°C.

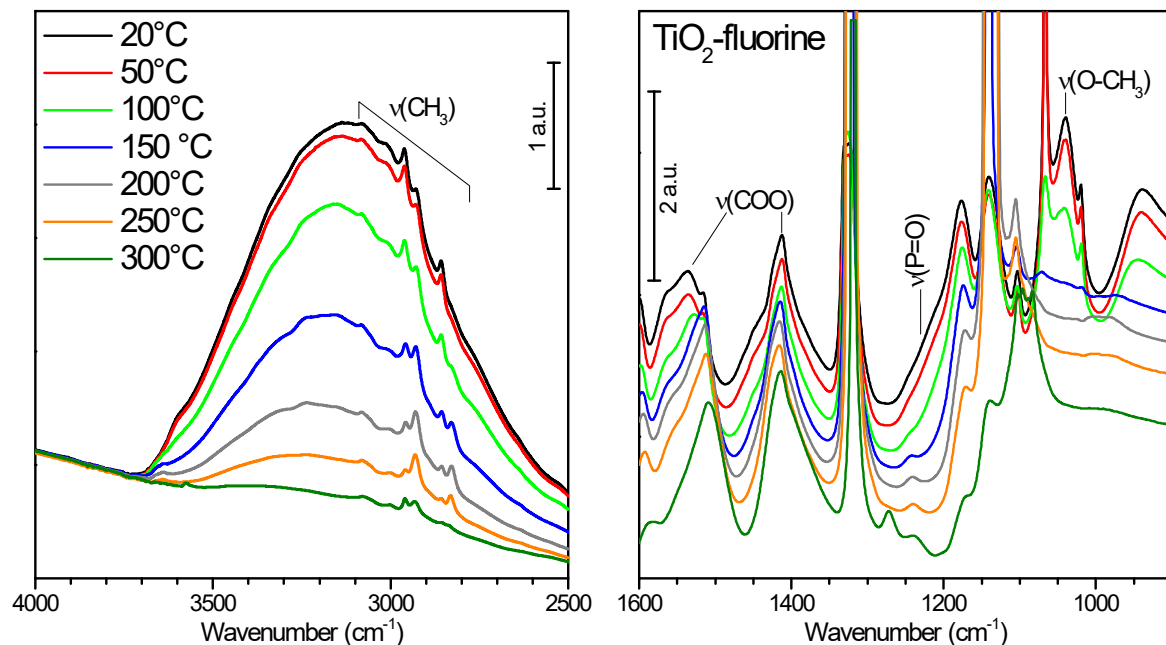


Figure S4: IR patterns of TiO_2 -fluorine recorded during the thermal programmed desorption between 20 and 300°C.

Role of water and interfering molecules

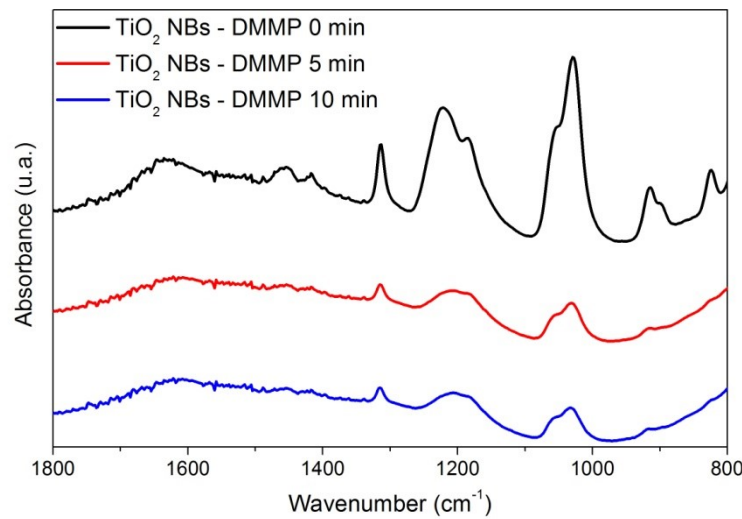


Figure S5: Evolution of IR signal measured by ATR on a Si surface nanostructured with TiO₂ NRs exposed in ambient air after exposition of concentrated DMMP vapour. At t=0 min, the sample is removed from the DMMP atmosphere IR spectra are recorded after 0, 5 and 10 min of air exposition.

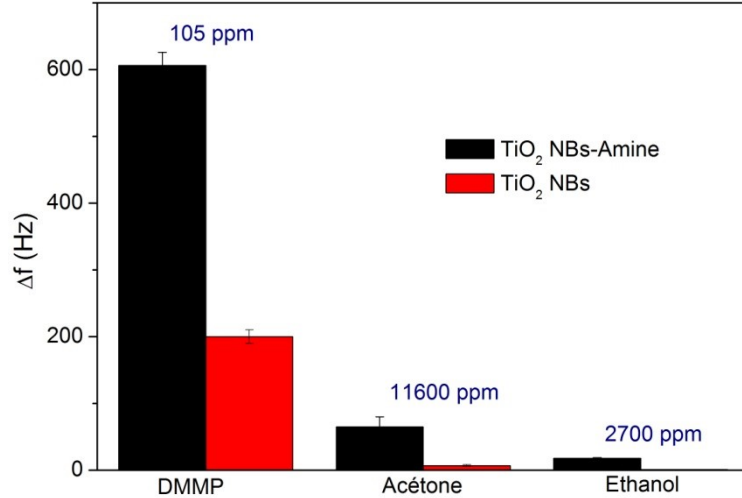


Figure S6: Response of a nanostructured microcantilever and a microcantilever nanostructured and functionalized with amino terminated molecules when exposed to 50 mL·min⁻¹ flow of air with DMMP, acetone or ethanol. Note that the concentrations of ethanol and acetone in air are order of magnitude higher than the one of DMMP.